

## Analysis on the effect of plasma and pyrolytic degradation in textile sludge

Rajendran M.<sup>1\*</sup>, Sivagami S. M.<sup>2</sup> & Aswin Sriram<sup>3,4\*</sup>

<sup>1</sup>Department of Mechatronics Engineering,

Hindusthan College of Engineering and Technology, Coimbatore, Tamil Nadu-641 032, India

<sup>2</sup>Alagappa Chettiar Government College of Engineering and Technology, Karaikudi, Tamil Nadu-630 003, India

<sup>3</sup>Department of Civil Engineering, and <sup>4</sup>Centre of Excellence in Water Research, Sri Sivasubramaniya Nadar College of Engineering, Rajiv Gandhi Salai (OMR), Kalavakkam, Tamil Nadu-603110, India

\*E-mail: gunnysiram@gmail.com (AS); rajenergypsg@gmail.com (RM)

Received 8 March 2024; accepted 17 September 2024

This investigation provides a comprehensive analysis of plasma-treated textile sludge, using scanning electron microscopy (SEM), energy dispersive X-ray spectroscopy, high-resolution transmission electron microscopy (HR-TEM), and thermogravimetric analysis (TGA) to uncover the material's microstructural, compositional, and thermal properties. SEM-EDX findings quantified the elemental makeup, revealing substantial quantities of calcium (29.76 wt%), oxygen (51.52 wt%), carbon (8.11 wt%), magnesium (10.19 wt%), and silicon (0.42 wt%), hinting at the formation of calcium-based minerals like calcite (CaCO<sub>3</sub>). HR-TEM analysis confirmed these findings through lattice spacings and diffraction patterns. The temperature profile reveals a range from approximately 27.60°C to 760.32°C, with a median temperature of 393.96°C. This systematic increase, followed by a decline, suggests a controlled heating and cooling cycle. The Differential Thermal Analysis exhibits variations between 1.87 μV and -28.73 μV, with pronounced peaks and troughs indicative of potential phase transitions or specific chemical reactions, shedding light on the sample's thermal stability and its endothermic or exothermic nature at distinct temperatures. The Thermogravimetric Analysis (shows a significant weight loss, starting from an initial weight of 4716.60 μg and reaching a minimum of 3761.88 μg, indicating a decomposition or volatilization of components. The Derivative Thermogravimetry (DTG) visualizes the rate of weight change, accentuating peaks as high as 51.68 μg/min and troughs plummeting to -44.48 μg/min. This study highlights how plasma treatment changes the sludge's structure and stability, offering useful insights for better waste management in the textile industry.

**Keywords:** Anomaly Detection, Derivative analysis, Plasma Degradation, Pyrolysis, Textile Sludge

### Introduction

Textile sludge, a byproduct of the wastewater treatment process in the textile industry, predominantly found in major textile manufacturing hubs like India, China, and Bangladesh, represents a significant environmental challenge due to its complex composition and the volume generated. This sludge is characterized by a mix of organic and inorganic substances. The organic fraction includes natural and synthetic fibers, oils, and greases, typically constituting about 30-60% of the dry weight of the sludge<sup>1</sup>. Inorganic constituents, which make up the remaining portion, primarily consist of metals and minerals. Notably, the sludge often contains hazardous substances like azo dyes, accounting for up to 70% of all dyes used in the industry, and heavy metals such as chromium, which can be present in concentrations up to 100 mg/kg in the dry sludge<sup>2</sup>. In terms of sludge volume ratios, the textile industry typically observes a range between 0.5% to 2% of the

volume of wastewater treated. The Mixed Liquor Suspended Solids (MLSS) concentration in these systems often lies within the 3000 to 6000 mg/L range, although this can vary based on operational practices and wastewater characteristics. The Biochemical Oxygen Demand (BOD) to Chemical Oxygen Demand (COD) ratio in textile sludge is a critical measure of its organic load and biodegradability. This ratio in textile sludge often falls below 0.3, considerably lower than in domestic sewage, indicating a higher proportion of non-biodegradable organic compounds. This is reflective of the complex and resistant nature of many dyes and chemicals used in textile processing. The hazardous nature of textile sludge is underscored by its content of toxic substances. Lead concentrations can reach up to 50 mg/kg, and cadmium levels can be as high as 20 mg/kg in the dry sludge<sup>3</sup>. Additionally, the presence of synthetic organic compounds poses risks to both aquatic ecosystems and human health through

potential soil and water contamination. Recent developments in the field have focused on the efficient management and treatment of textile sludge. Efforts are directed towards reducing the volume of sludge generated through optimized water usage and improved wastewater treatment technologies. Furthermore, research into sludge valorization is gaining momentum, with studies exploring the conversion of sludge into construction materials or energy via incineration, pyrolysis, and gasification<sup>4</sup>. These methods not only help in managing the environmental impact of the sludge but also offer potential economic benefits by transforming waste into valuable resources.

Plasma degradation of sludge, an advanced waste treatment technology, involves the use of plasma - a highly ionized gas with energetic particles - to break down organic and inorganic constituents in sludge<sup>5</sup>. This method is increasingly recognized for its efficiency in treating various types of waste, including the complex and hazardous sludge generated by industries such as textiles. In plasma degradation, the sludge is exposed to high temperatures, typically ranging from 3,000 to 8,000 K, generated by an electric arc, radio frequency, or microwave-induced plasma. This process leads to the pyrolysis and gasification of organic matter. The high temperature ensures complete breakdown of complex molecules into simpler forms, often resulting in a mixture of hydrogen, carbon monoxide, and trace amounts of other gases<sup>6</sup>. The process is driven by the thermal and chemical energy of the plasma. Electrons in the plasma have enough energy to break chemical bonds, leading to the destruction of hazardous compounds like dioxins and furans, which are commonly found in industrial sludge. Plasma treatment can achieve a degradation efficiency of up to 99.99% for these compounds. Furthermore, heavy metals present in the sludge are immobilized or converted into less harmful forms, reducing their environmental impact. Key operational parameters in plasma degradation include the type of plasma generator used, power input, treatment time, and the nature of the sludge<sup>7</sup>. For instance, the power input can vary from a few kilowatts to several megawatts, depending on the scale and desired efficiency of the process. Treatment time can range from a few seconds to several minutes, influenced by the composition and volume of the sludge. Compared to conventional thermal treatments like incineration, plasma

degradation offers several advantages. It operates at higher temperatures, ensuring more complete breakdown of complex molecules. The process also has a smaller footprint and produces fewer emissions, particularly lower levels of CO<sub>2</sub>, NO<sub>x</sub>, and SO<sub>x</sub>, due to the contained and controlled nature of the plasma environment. One of the main challenges in plasma degradation is the high energy requirement, which can impact the overall cost-effectiveness of the process<sup>8</sup>. Recent advancements in plasma technology aim to enhance energy efficiency and scalability. There is ongoing research into hybrid systems that combine plasma with other treatment methods, like catalysis, to improve efficiency and reduce costs. Additionally, studies are exploring the recovery of energy and materials from the process, such as the synthesis of syngas (a mixture of hydrogen and carbon monoxide) for energy production.

Plasma degradation and pyrolysis, both employed for biomass degradation, exhibit distinctive operational characteristics, efficiencies, and environmental impacts. Plasma degradation uses highly energetic, ionized gases in a plasma state, generated through electrical energy. This method is highly efficient in breaking down complex organic molecules, and is effective in neutralizing or immobilizing hazardous elements like heavy metals<sup>9</sup>. Pyrolysis, on the other hand, involves thermal decomposition of biomass in an inert or oxygen-limited environment, usually between 400 and 800°C. It yields a variety of products including biochar, bio-oil, and syngas, with the specific output ratios dependent on factors like temperature and biomass composition<sup>10</sup>. While plasma degradation demands higher energy inputs due to its reliance on electricity for plasma generation, making it cost-intensive, it offers the benefit of lower emissions. Pyrolysis, less energy-consuming than plasma degradation, may have higher emission levels if its by-products, such as bio-oil and syngas, are not efficiently utilized. Recent advancements in plasma degradation aim at improving energy efficiency and scalability, incorporating hybrid methods that combine plasma with other treatment technologies<sup>11</sup>. Innovations in pyrolysis focus on optimizing reactor designs and processing conditions to enhance the quality and yield of bio-oil and syngas, and the production of biochar for applications like soil amendment and carbon sequestration<sup>12</sup>. Ultimately, the selection between plasma degradation and pyrolysis depends on the

specific waste characteristics, desired end-products, and economic viability, with each offering unique advantages in biomass degradation- plasma degradation with its high efficiency and environmentally friendly profile, and pyrolysis with its versatility in biomass valorization and potential for renewable energy production<sup>13-14</sup>.

### Experimental Section

In this study, a comprehensive investigation was conducted into the gasification of textile sludge obtained from a wastewater treatment facility in the Tirupur District, South India. The textile sludge was collected post-wastewater treatment from dyeing industries. Initial characterization involved analytical and gas chromatographic analyses, along with X-ray diffraction (XRD), to determine its composition, which included organic matter, micronutrients, dyes, heavy metals, and pathogenic microorganisms. For the gasification process, the sludge was pre-dried to minimize moisture content, thereby reducing exergetic losses during treatment. The dried sludge was then formed into pellets using PVC binders to ensure stability within the plasma chamber and prevent dislodgement during treatment. The gasification experiments utilized a single chamber reactor, chosen over a two-stage process for its simplicity and efficiency. An equilibrium model was formulated to establish the thermodynamic limits of the process, and energy balance equations were developed to guide the experimental setup. The targeted gasification temperature was set at a minimum of 600°C to ensure optimal reaction conditions. The plasma treatment employed non-equilibrium DC non-transferred plasma torches with water-cooled electrodes. The apparatus comprised graphite crucibles and electrodes, alongside an electrical supply system. The chamber, constructed of bricks and steel, was designed to withstand the high temperatures and intense conditions of plasma treatment. The weight of the sludge was meticulously recorded before and after treatment to assess mass loss and treatment efficacy. The experimental runs were conducted under various conditions to study the effects of different gas combinations and sludge treatment processes. The collected data included changes in weight, gas compositions, and other qualitative characteristics of the treated sludge. This comprehensive approach allowed for a detailed understanding of the plasma gasification process, including its efficiency and the

impact of different operational parameters on the treatment outcome.

High-Resolution Transmission Electron Microscopy (HRTEM) and Scanning Electron Microscopy with Energy Dispersive X-ray Analysis (SEM-EDX) were employed to analyze both plasma-treated and untreated textile sludge samples. The HRTEM analysis was pivotal in revealing the nanoscale structural alterations in the sludge. Prior to imaging, we prepared the samples by drying and finely grinding them to ensure uniformity. A suspension was created by dispersing a small amount of the powdered sample in ethanol, followed by ultrasonication. This suspension was then deposited onto a carbon-coated copper grid and allowed to dry in a desiccator. Using HRTEM, we observed the samples at various magnifications. The focus was on identifying morphological changes and shifts in crystallinity, especially in the plasma-treated sludge. This comparative analysis between treated and untreated samples elucidated the physical modifications induced by plasma treatment, like alterations in particle size, shape, and aggregation. For SEM-EDX analysis, we first dried the sludge samples and then coated them with a conductive layer of gold using a sputter coater. This coating was essential to prevent electron beam charging during examination. In the SEM analysis, a focused electron beam was scanned over the sample surface, generating high-resolution images that revealed surface textures, pore structures, and morphological features. The EDX component was crucial for elemental analysis. By bombarding the samples with electrons and measuring the emitted characteristic X-rays, we quantified elemental composition changes resulting from plasma treatment. This analysis was particularly instrumental in assessing the transformation or reduction of heavy metals and other hazardous components in the sludge. The combination of HRTEM and SEM-EDX analyses provided a thorough understanding of the effects of plasma treatment on textile sludge. The HRTEM analysis highlighted nanoscale structural changes, while SEM-EDX offered detailed insights into surface morphology and compositional shifts, underpinning the efficacy and implications of plasma treatment in altering the sludge's characteristics.

### Results and Discussion

#### Thermogravimetric data analysis

The thermal behaviour of a sample over the experimental period with respect to time and

temperature is shown in Fig. 1. The temperature profile reveals a range from approximately 27.60°C to 760.32°C, with a median temperature of 393.96°C. This systematic increase, followed by a decline, suggests a controlled heating and cooling cycle. The Differential Thermal Analysis (DTA) exhibits variations between 1.87  $\mu\text{V}$  and  $-28.73 \mu\text{V}$ . These pronounced peaks and troughs in the "DTA vs. Time" graph are indicative of potential phase transitions or specific chemical reactions, shedding light on the sample's thermal stability and its endothermic or exothermic nature at distinct temperatures<sup>15</sup>. The "TG vs. Time" graph reflects a sample weight ranging from 4716.60  $\mu\text{g}$  to 3761.88  $\mu\text{g}$ , signifying a decomposition or volatilization of components. The "DTG vs. Time" visualization, representing the rate of weight change, accentuates this with peaks reaching as high as 51.68  $\mu\text{g}/\text{min}$  and troughs plummeting to  $-44.48 \mu\text{g}/\text{min}$ . The "TG vs. Time" graph provides a comprehensive view of the sample's weight over the course of the thermal experiment. The sample starts at an initial weight of approximately 4716.60  $\mu\text{g}$ . As time progresses, a systematic decrease in weight is observed, reaching a minimum of 3761.88  $\mu\text{g}$ . This weight loss, amounting to almost 954.72  $\mu\text{g}$ , signifies a potential decomposition or volatilization of components within

the sample<sup>16</sup>. Such weight losses can be attributed to the release of bound water, organic volatiles, or other volatile components that escape upon heating. The "DTG vs. Time" visualization further augments our understanding of this behavior<sup>17</sup>. DTG, representing the rate of weight change, showcases moments of heightened reactivity or significant phase shifts in the sample. Peaks reaching as high as 51.68  $\mu\text{g}/\text{min}$  indicate rapid weight losses, possibly due to fast-evolving gaseous products or swift decomposition reactions. On the other hand, troughs plummeting to  $-44.48 \mu\text{g}/\text{min}$  spotlight moments of reduced reactivity. The oscillations in the DTG curve, with its pronounced peaks and troughs, suggest the occurrence of multiple thermal events or reactions over the experimental timeline<sup>18</sup>.

#### Correlation analysis

The TGA dataset can be analysed through three different correlation parameters namely Pearson Coefficient ( $r$ ), Spearman's Rank Correlation Coefficient ( $\rho$ ) and Kendall's Tau Coefficient ( $\tau$ ). The Pearson Coefficient is determined by the following equation as presented below in Eq. (1). The characteristic trait of the Pearson Coefficient is that (i) Measures the linear relationship between two

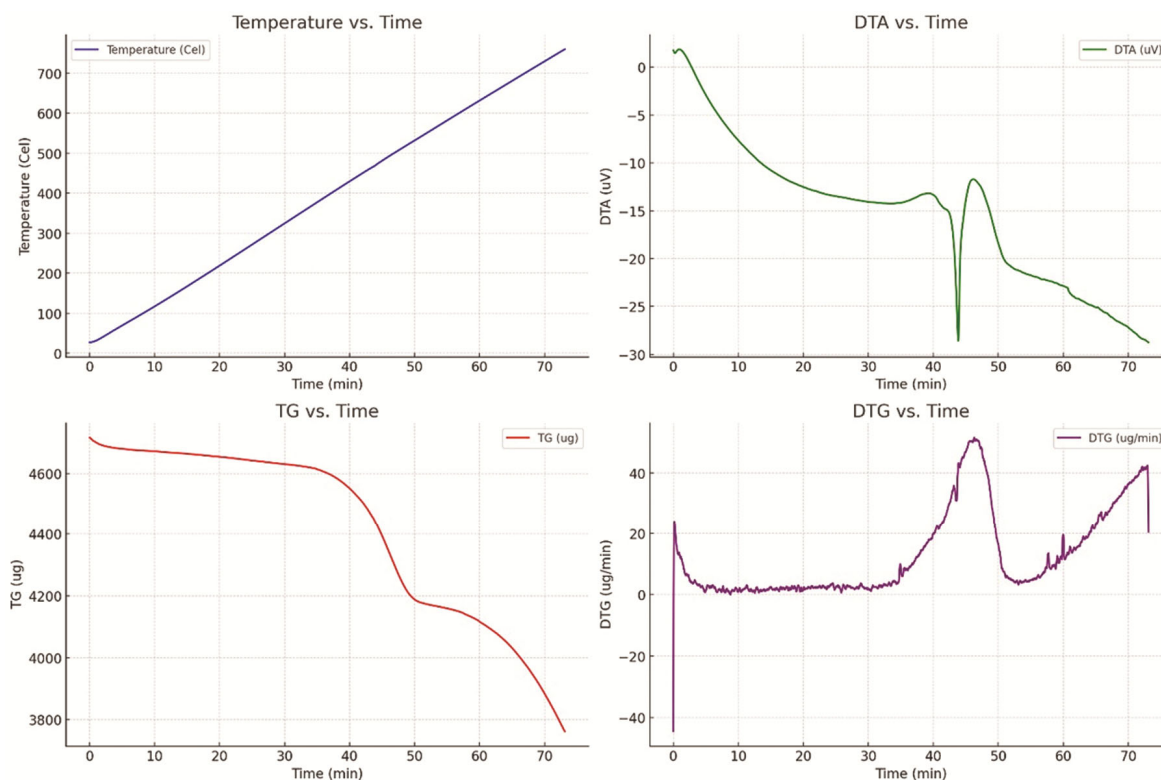


Fig. 1 — TGA variation of Textile Sludge with reference to incremental temperature variation

datasets and (ii) it assumes the datasets are normally distributed.

$$r = \frac{\sum_{i=1}^n (x_i - \bar{x})(y_i - \bar{y})}{\sqrt{\sum_{i=1}^n ((x_i - \bar{x})^2) \sum_{i=1}^n ((y_i - \bar{y})^2)}} \quad \dots (1)$$

The Pearson correlation coefficient measures the linear relationship between two datasets. A value close to -1 suggests a strong negative linear relationship. For "Temperature vs. DTA", the coefficient of -0.941 indicates a strong inverse linear relationship, which means as the temperature rises, the DTA values tend to decrease<sup>19</sup>. For "Temperature vs. DTG", a coefficient of 0.618 suggests a moderate positive linear relationship. The Spearman's Rank Correlation Coefficient measures the monotonic relationship between two datasets. It does not assume the datasets are normally distributed and they are based on ranked values rather than the raw data. The Spearman's Rank Correlation Coefficient is calculated through the following equation as represented in Eq. (2).

$$r_s = 1 - \frac{6 \sum d_i^2}{n(n^2 - 1)} \quad \dots (2)$$

Spearman's correlation assesses how well the relationship between two variables can be described using a monotonic function. The coefficient for "Temperature vs. DTA" is -0.947, suggesting a strong negative monotonic relationship. For "Temperature vs. DTG", a coefficient of 0.738 indicates a strong positive monotonic relationship. Similarly, the Kendall's Tau Coefficient ( $\tau$ ) measures the ordinal association between two datasets. Like Spearman, it's based on ranks and it calculates the difference between the number of

concordant and discordant pairs. The Kendall's Tau Coefficient ( $\tau$ ) is calculated through the following equation as represented in Eq.3.

$$\tau = \frac{n_c - n_d}{\frac{1}{2}n(n-1)} \quad \dots (3)$$

Kendall's Tau measures ordinal associations between two datasets. The coefficient for "Temperature vs. DTA" is -0.877, suggesting a strong ordinal association such that as one variable increases, the other tends to decrease. For "Temperature vs. DTG", a coefficient of 0.566 indicates a moderate positive ordinal association.

**Cumulative weight Gain**

The cumulative weight loss or gain over time can be derived from the DTG (rate of weight change) data as shown in Fig. 2. By integrating the DTG curve over time, we can determine the total weight change at each time point. The thermal behavior of the sample was analyzed with a focus on its cumulative weight change over the experimental duration. The sample showed a total weight loss of approximately 953.55  $\mu\text{g}$ . The maximum cumulative weight change occurred at 73.13 min and the minimum was observed at 0.03 min. The data revealed a rate of cumulative weight change, and its correlation with the sample's temperature was found to be 0.929. This strong positive correlation indicates that as the temperature of the sample increased, the cumulative weight change also increased<sup>20</sup>. By comparing the rate of cumulative change with the immediate weight change rates (DTG), periods of stability were identified. During these periods, the sample's weight remained relatively constant. Additionally, inflection points

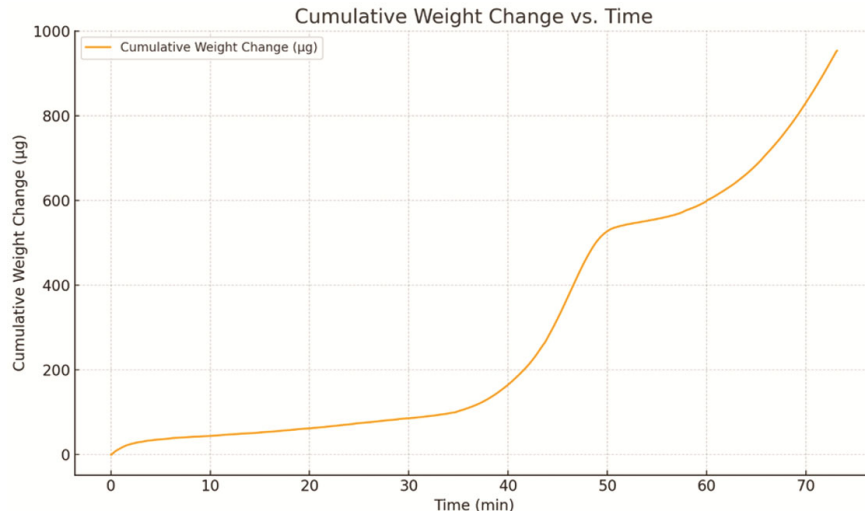


Fig. 2 — Cumulative weight Change plot against time variation for Textile Sludge

were identified at specific time intervals, suggesting transitions in the sample's behavior due to different thermal events or reactions.

#### **Anomaly detection**

Anomaly detection is the process of identifying unusual patterns that do not conform to expected behaviour. It's a crucial step in many data analysis tasks, as identifying these anomalies can lead to significant insights or indicate potential issues with the data or the system under study. There are various techniques for anomaly detection. Given the nature of the TGA dataset (time-series data with multiple features), we can employ the following methods, viz. a) Statistical Methods – which involves checking if data deviates significantly from a statistical distribution and Z-score is a common method, where values that are too far from the mean are treated as anomalies, b) Isolation Forest – which is a tree-based anomaly detection algorithm and it isolates anomalies by splitting the data recursively and identifying points that are isolated with fewer splits, and c) One-Class SVM (Support Vector Machine) – which is an algorithm learns a soft boundary to cluster the normal data and identifies data points outside this boundary as anomalies.

#### ***Isolation Forest method and its application to the TGA dataset***

The Isolation Forest algorithm is an anomaly detection technique that fundamentally operates by isolating observations. Unlike traditional methods that measure the normality of data points, Isolation Forest focuses on isolating anomalies. The core principle is that anomalies are data points that are few and different, and thus, they can be easily isolated from the rest. The algorithm works by constructing multiple decision trees. In each tree, a feature is randomly selected, and a random split value between the minimum and maximum value of the selected feature is defined. This process is recursively repeated until data points are isolated or trees reach a certain depth. Anomalies are data points that have short paths in the trees, meaning they are isolated quicker than regular points. For the current study of the TGA dataset as shown in Fig. 3, which comprises features like temperature, DTA, TG, and DTG, the Isolation Forest algorithm was applied to discern data points that deviate from expected patterns. These deviations could represent measurement errors, unusual reactions, or significant thermal events.

The identified anomalies were then visualized on the respective feature vs. time plots, offering insights

into potential outlier behavior over the experimental duration. A recent study offered a comprehensive exploration into the realm of anomaly detection<sup>21</sup>. Their research centred on an extension to the model-free anomaly detection algorithm, originally known as the Isolation Forest. The developed extension was termed as the Extended Isolation Forest (EIF). A significant motivation for the inception of EIF was the observed challenges associated with the assignment of anomaly scores to specific data points in the original Isolation Forest algorithm. One of the pivotal tools employed in the research to illustrate these challenges was the heat map for anomaly scores. The heat maps revealed artifacts that were previously unnoticed, and these artifacts were attributed to the tree branching mechanism inherent in the original algorithm. The Extended Isolation Forest was thus presented as a remedy to these observed biases, promising a more accurate and robust anomaly detection mechanism. The extended model, rooted in the concept of binary trees, has been highlighted for its potential in anomaly detection applications. The binary tree structure, a foundation of the model, allows for efficient detection of anomalies, combining linear time complexity with minimal memory usage. While the original Isolation Forest algorithm was recognized for its innovative approach to detection, the Extended Isolation Forest has been presented as an enhanced version, aiming to overcome the biases and limitations of its predecessor.

The Isolation Forest and Extended Isolation Forest are both innovative algorithms designed for anomaly detection, but they have distinct characteristics and methodologies. The original Isolation Forest determines anomalies based on the branching structure of trees. In this method, anomalies are typically isolated closer to the root of the tree, requiring fewer splits to identify them. However, this method exhibits a certain bias due to its tree branching mechanism. On the other hand, the Extended Isolation Forest (EIF) offers a solution to this bias. In the standard Isolation Forest, branching is based on axis-aligned splits. In contrast, EIF introduces a more versatile approach, allowing branching to occur in every possible direction. This enhancement in EIF not only offers a more robust detection mechanism but also resolves specific issues related to the assignment of anomaly scores to data points. By doing so, EIF provides a more accurate representation of the anomalous nature of the data. When applied to a TGA (Thermogravimetric Analysis)

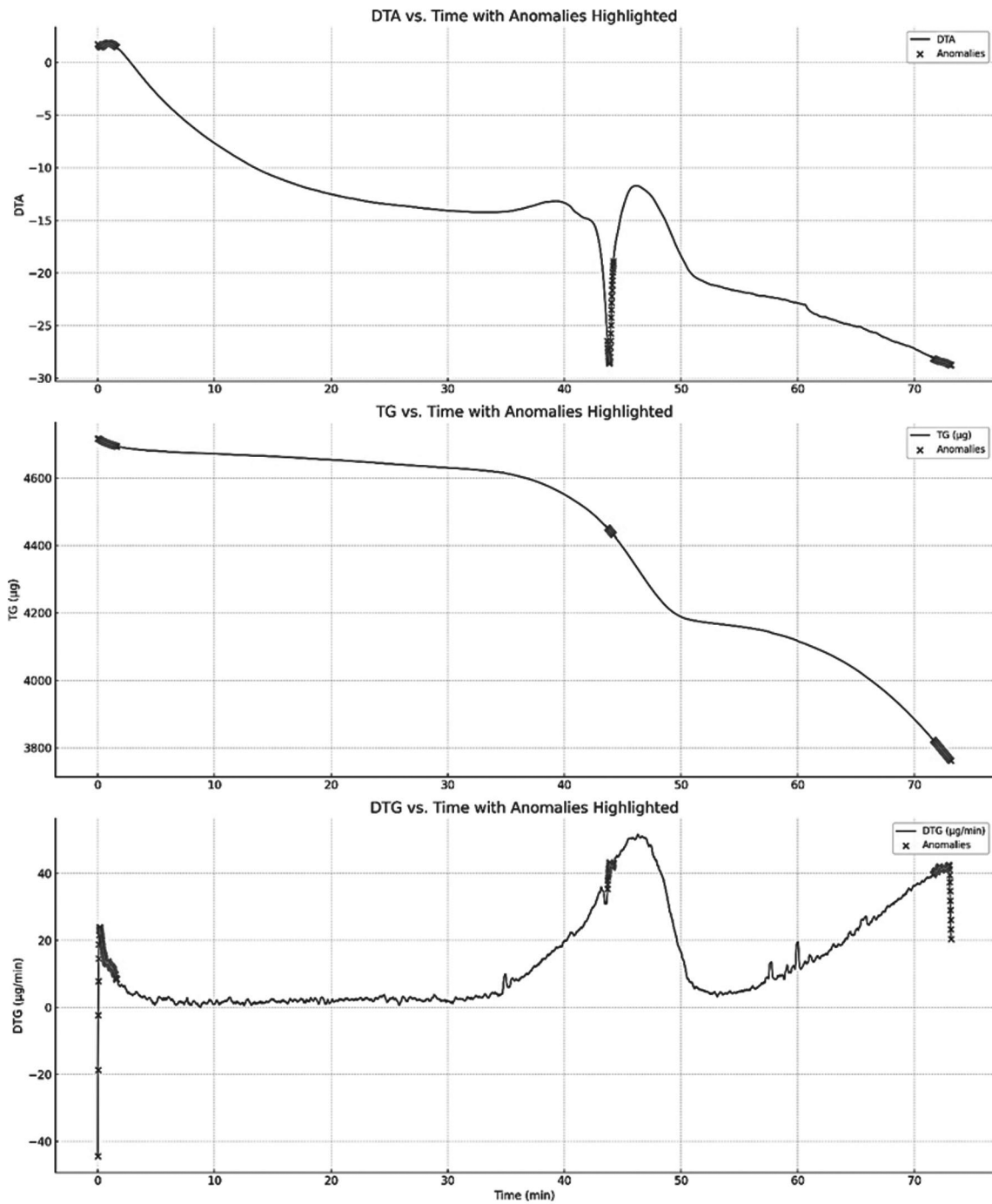


Fig. 3 — Anomaly detection through Isolation Forest method for TGA-DTA of the Textile Sludge sample

vs time plot, the choice between these two methods largely depends on the specific characteristics of the data and the objectives of the analysis. Given that TGA data can have intricate features depending on the material being analyzed, the Extended Isolation Forest might offer a more nuanced and reliable detection of anomalies or unexpected behaviors in the data compared to the standard Isolation Forest. However, the actual accuracy

would depend on the specific dataset and the nature of the anomalies present. The Isolation Forest algorithm recursively partitions the data space by randomly selecting a feature and then randomly selecting a split value between the minimum and maximum values of the selected feature. This random partitioning produces shorter paths for anomalies since the chances of isolating anomalies are higher. Once the trees are constructed, the

path length (i.e., the number of edges an observation must pass in the tree going from the root to the terminal node) is used as a measure of normality. Shorter paths indicate anomalies. The anomaly score is derived based on the path length. It is a measure of how isolated an observation is relative to the rest of the data. While Extended Isolation Forest retains the core concepts of the original method, it introduces modifications to address certain biases. Instead of using axis-aligned splits as in the original method, Extended Isolation Forest employs random hyperplanes to partition the data space. This allows the branching process to occur in every direction, providing a more generalized approach. The method resolves some issues with the assignment of anomaly scores, making them more consistent and reliable.

#### *K-means isolation test*

A novel method known as the K-Means Isolation Test was introduced in a recent study, which combined the principles of the K-Means clustering algorithm with the Isolation Forest technique for anomaly detection<sup>22</sup>. The primary motivation was to enhance the efficiency and accuracy of anomaly detection, especially in large datasets, by leveraging the strengths of both the mentioned algorithms. The K-Means clustering algorithm is traditionally employed for partitioning datasets into clusters based on similarity. In this research, the K-Means algorithm was used to initially segregate the data into clusters, thus reducing the dimensionality and complexity of the dataset<sup>23</sup>. Following this, the Isolation Forest technique known for its ability to detect anomalies by isolating them, is applied to each cluster. This sequential approach not only aids in pinpointing the anomalies with higher precision but also in reducing the computational burden, making it well-suited for big data applications. The TGA data was first segmented into three distinct clusters using the K-Means algorithm, grouping data points with similar characteristics based on the provided features. Within these individual clusters, an anomaly detection technique, the Isolation Forest, was then applied. Cluster 0 had 13 detected anomalies, Cluster 1 had 8, and Cluster 2 had 7. Interestingly, Cluster 0 exhibited a marginally higher number of anomalies compared to the other clusters. This suggests that the data points in Cluster 0 might either encompass a broader range of values or have specific points that diverge notably from the cluster's general trend. The use of the K-Means Isolation approach offers a layered method to anomaly detection. By clustering the data initially, it allows for

the recognition of local patterns and trends within each segment, potentially providing a more precise identification of anomalies than if a universal technique was applied to the entire dataset. The pinpointed anomalies in the clusters as shown in Fig. 4 warrant further examination to discern if they are genuine outliers, errors in measurement, or other unique occurrences that could be of investigative interest.

#### **Peak analysis**

Peak analysis involves identifying significant maxima in the data which can represent specific reactions or phase changes in thermogravimetric analysis (TGA). For the "TG vs. Time" curve, distinct peaks represent significant weight changes, possibly due to phase transitions or chemical reactions. The "DTG vs. Time" curve, being the derivative of the TG curve, displays peaks at the points of maximum rate of weight change, corresponding to the most active thermal events in the sample. Our analysis pinpointed several such peaks, indicating multiple significant events during the sample's thermal decomposition. In thermogravimetric analysis, peaks are often representations of significant thermal events, such as evaporation, sublimation, oxidation, or decomposition. The prominence of each peak can give insight into the magnitude or significance of the corresponding event. For the "TG vs. Time" curve, observing peaks provides insights into weight changes at specific temperature ranges. These changes could be attributed to loss or gain of volatile components, breakdown of organic compounds, or other chemical transformations. The specific temperature at which these peaks occur can be indicative of the stability or reactivity of the material. The "DTG vs. Time" curve is particularly insightful as it highlights the rate of these weight changes. A pronounced peak in the DTG curve indicates a rapid weight change, signaling an intense

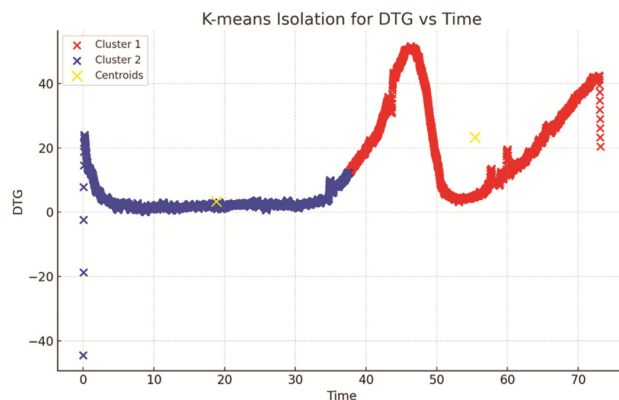


Fig. 4 — Anomaly detection through K-Means Isolation method for DTG – time plot of the Textile Sludge sample

thermal event or reaction. Multiple peaks in succession can suggest a sequence of reactions or transformations that the sample undergoes.

**Rate of change**

The rate of change or the derivative provides insights into the velocity of a particular event or reaction. In the context of TGA, for the "TG vs. Time" curve, the rate of change gives us the weight change rate over time, while for the "DTG vs. Time" curve, it provides the acceleration or the second derivative of weight with respect to time. Monitoring these rates can reveal periods of rapid change and help in understanding the kinetics of thermal decomposition. Understanding the rate of change in a TGA curve can provide a quantitative measure of the kinetics of thermal events. For instance, a steadily increasing rate could indicate a cumulative or synergistic effect of multiple reactions<sup>24</sup>. In the "TG vs. Time" curve, the rate of change signifies how quickly the sample is gaining or losing weight. A high positive rate indicates rapid weight gain, while a high negative rate suggests rapid weight loss. Such rates can be linked to processes like absorption, desorption, or chemical reactions that either produce or consume material. The second derivative, as visualized in the "DTG vs. Time"

curve, captures the acceleration or deceleration of these weight changes. A peak in this curve, for instance, can indicate the point of maximum reaction rate, which can be pivotal in understanding reaction kinetics and mechanisms.

**Phase transition analysis**

Phase transitions in TGA are typically marked by abrupt changes in weight or sharp peaks in the derivative. The "TG vs. Time" curve can display sudden drops or rises, indicating phase transitions, while the "DTG vs. Time" curve, being the derivative, will exhibit pronounced peaks at these junctures. By juxtaposing the data with the identified peaks, our analysis aimed to highlight potential phase transitions in the sample. These transitions could be due to processes like dehydration, sublimation, or chemical decomposition. Phase transitions, in the context of TGA, are marked by abrupt changes in the weight of the sample. Such changes can be due to physical processes like the melting of a solid or the boiling of a liquid, or chemical processes like the decomposition of a compound.

In the "TG vs. Time" curve as shown in Fig. 5, the sudden drops or plateaus indicate phase transitions. For instance, a rapid weight loss could be due to the sample

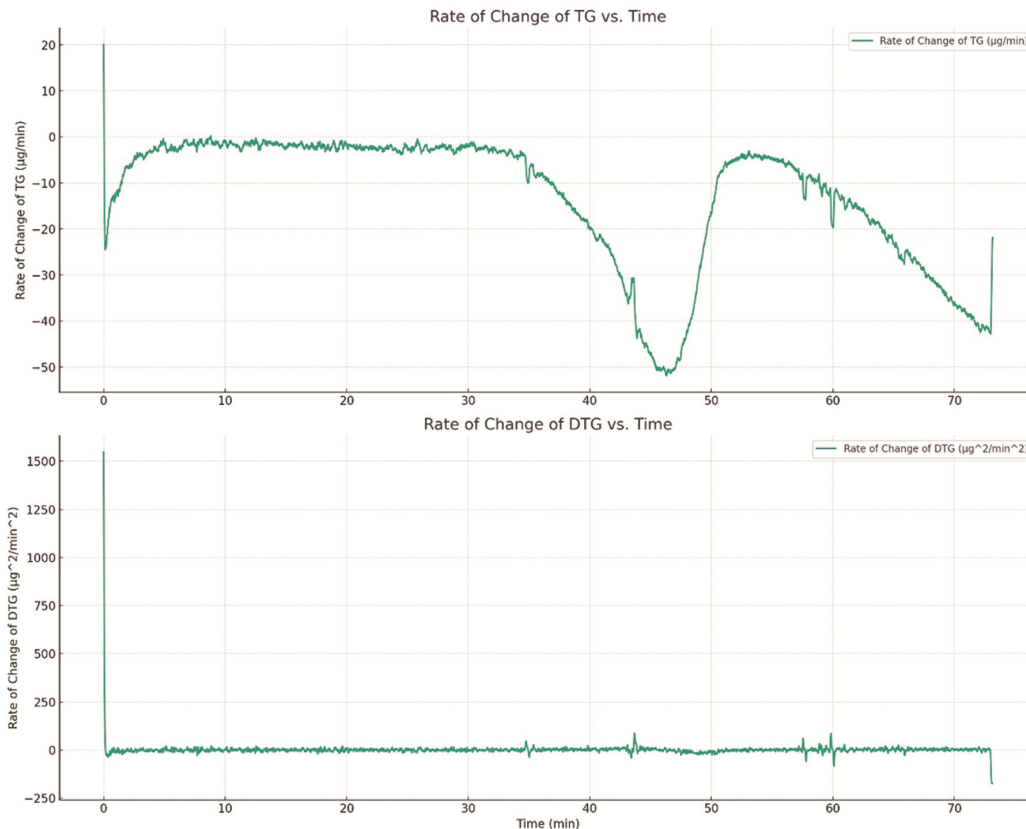


Fig. 5 — Phase transition analysis for DTG – time plot of the Textile Sludge sample

undergoing sublimation or releasing a volatile component. On the other hand, a plateau or region of stability can suggest the material's resilience to change over that temperature range. The "DTG vs. Time" curve enhances this analysis by pinpointing the exact temperatures at which these phase transitions occur, as evidenced by sharp peaks. By correlating these peaks with known phase transition temperatures, one can deduce the nature of the sample and its components<sup>25</sup>.

### Structural analysis

In the HR-TEM analysis of the plasma-treated textile sludge, high-resolution images revealed detailed microstructural characteristics of the sample at the nanoscale. The HR-TEM images displayed a variety of crystallographic features, including lattice fringes and diffraction patterns indicative of crystalline phases. Notably, areas within the HR-TEM images showed periodic lattice spacings, suggesting the presence of specific crystalline minerals. Given the chemical composition data obtained from complementary EDX analysis, which indicated significant amounts of calcium, oxygen, and carbon, the HR-TEM findings were cross-referenced with known crystalline structures. This comparison suggested the presence of calcite ( $\text{CaCO}_3$ ) within the sample, a conclusion supported by characteristic lattice spacings observed in the HR-TEM images as shown in Fig. 6. These microstructural observations are consistent with the expected

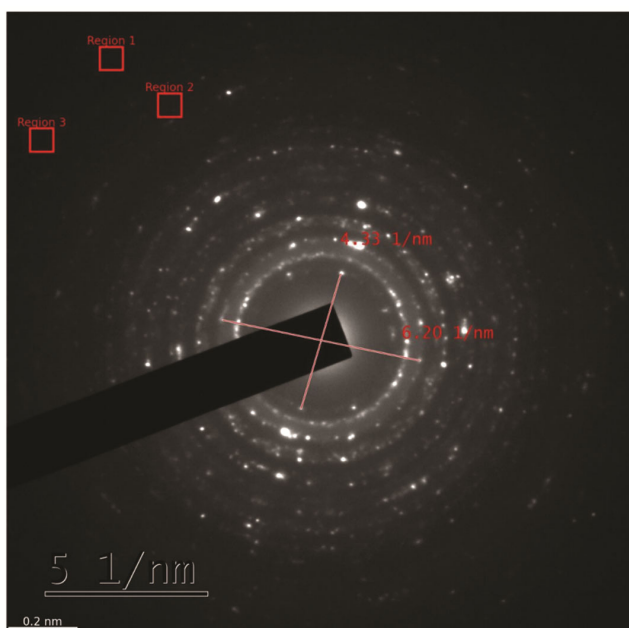


Fig. 6 — HR-TEM image of the Plasma treated Textile Sludge

outcomes of high-temperature plasma treatment processes, which can induce crystallization or phase transformations in treated materials. The HR-TEM analysis, therefore, provided crucial insights into the nano-scale structural composition of the plasma-treated textile sludge, highlighting the formation of calcite as a result of the treatment process.

SEM analysis of the plasma-treated textile sludge unveiled a diverse surface morphology characterized by granulated structures and surface roughness and is shown in Fig. 7. These morphological features underscore the complex interplay of materials and potential phase transformations induced by the plasma treatment. Complementing the SEM findings, the Energy Dispersive X-ray Spectroscopy (EDX) analysis elucidated the sample's elemental composition, revealing a predominant presence of calcium (29.76 wt%), oxygen (51.52 wt%), and carbon (8.11 wt%), along with minor constituents such as magnesium (10.19 wt%) and silicon (0.42 wt%). The substantial calcium concentration, coupled with the observed carbon and oxygen levels, strongly indicates the formation of calcium-based compounds, most notably calcite ( $\text{CaCO}_3$ ), within the treated sludge. This inference is bolstered by the SEM imagery, which showed structures resembling the rhombohedral crystalline form of calcite. Furthermore, the EDX data's identification of magnesium and silicon points towards the potential presence of additional mineral phases, enriching the sample's compositional complexity. Altogether, the SEM and EDX analyses provide a detailed portrayal of the surface characteristics and elemental distribution in the sample, affirming the hypothesis that plasma treatment promotes the

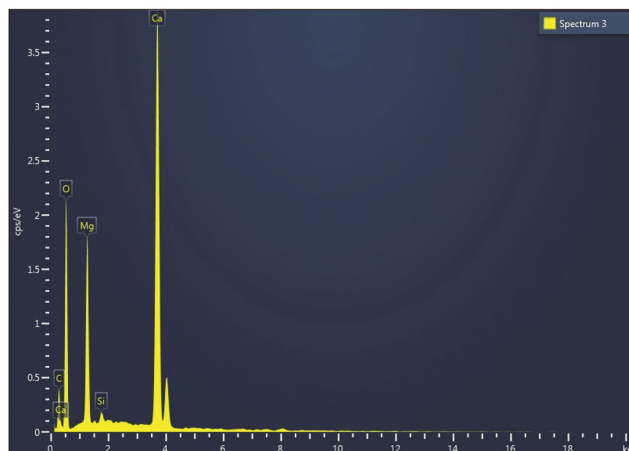


Fig 7 — SEM-EDX pattern image of the Plasma treated Textile Sludge

crystallization or formation of specific mineral phases such as calcite, along with a suite of other compounds.

The methods employed in this study, including Scanning Electron Microscopy (SEM), Energy Dispersive X-ray Spectroscopy (EDX), High-Resolution Transmission Electron Microscopy (HR-TEM), and Thermogravimetric Analysis (TGA), each offer distinct advantages and limitations. SEM provides detailed surface morphology, allowing for the visualization of granulated structures and surface roughness, which are crucial for understanding the physical transformations in plasma-treated sludge. However, SEM's limitation lies in its inability to provide information about the internal structure or chemical composition beyond the surface. EDX complements SEM by offering elemental composition analysis, but its accuracy can be affected by the sample's surface roughness and the depth of X-ray penetration, potentially leading to errors in quantification. HR-TEM excels in revealing nanoscale structural details and crystallographic features, making it invaluable for identifying specific crystalline phases like calcite. Nevertheless, HR-TEM is limited by its complexity, the need for extensive sample preparation, and the potential for beam-induced damage, which can alter the sample's original structure. TGA is instrumental in analyzing the thermal stability and decomposition behavior of the sludge, providing quantitative data on weight loss and phase transitions. However, TGA's limitation is its inability to distinguish between overlapping thermal events or identify the specific chemical compounds responsible for weight changes, often requiring complementary analytical techniques for a complete understanding. Together, these methods provide a comprehensive view of the plasma-treated sludge's properties, but they also highlight the necessity of combining different techniques to overcome individual limitations.

In the present study, various data analysis methods were employed to interpret the results comprehensively. The Pearson Correlation Coefficient was utilized to measure the strength and direction of the linear relationship between variables. Its advantage lies in its simplicity and ability to clearly define linear relationships, which is particularly useful when analyzing thermal stability or decomposition patterns in the textile sludge. However, its limitation is noted in its restriction to linear relationships, potentially missing non-linear patterns, and its sensitivity to outliers, which could distort the results in the context of complex material behavior. The Spearman's Rank Correlation Coefficient was applied to assess monotonic

relationships between variables, offering the advantage of not requiring normally distributed data and being more robust against outliers compared to Pearson's. This makes it suitable for analyzing rank-based relationships in the data, such as temperature variations and their effects on material properties, though it may still not effectively capture non-linear relationships.

Kendall's Tau Coefficient was employed to measure the ordinal association between variables, proving particularly useful in cases of small sample sizes or when the data is strongly tied to ranks. This method provides a more accurate measure of ordinal relationships than Spearman's in certain situations, but it also shares the limitation of not handling non-linear relationships well and may offer less interpretative power when the data lacks a clear ordinal structure. For the detection of unusual patterns, Anomaly Detection techniques, including the Isolation Forest algorithm, were employed. These methods are crucial for identifying outliers that may indicate significant material behavior under plasma treatment. The Isolation Forest method is particularly effective in complex, high-dimensional datasets due to its design for isolating anomalies through random data partitioning. However, the potential for biases in anomaly scoring and the need for careful tuning to the specific dataset characteristics were noted as limitations. Overall, these methods provided a comprehensive analytical framework, enabling detailed insights into the relationships, trends, and anomalies within the data, although each method also presented certain limitations that were mitigated through the complementary use of multiple techniques.

## Conclusion

In this study, sophisticated analytical techniques including Scanning Electron Microscopy (SEM), Energy Dispersive X-ray Spectroscopy (EDX), High-Resolution Transmission Electron Microscopy (HR-TEM), and Thermogravimetric Analysis (TGA) were employed to analyze plasma-treated textile sludge. SEM analysis unveiled a granulated texture and surface roughness, while EDX identified significant calcium (29.76 wt%), oxygen (51.52 wt%), and carbon (8.11 wt%) content, suggesting the formation of calcite ( $\text{CaCO}_3$ ), as confirmed by HR-TEM through lattice spacings and diffraction patterns consistent with calcite's structure. TGA revealed thermal events indicative of decomposition and phase transitions, pinpointing the dynamic thermal behavior of the sample. The integration of these analyses provided a detailed understanding of the sample's composition and thermal properties,

highlighting the transformative effect of plasma treatment on the sludge's microstructure and stability. The statistical analysis in the present study primarily involved the application of various correlation coefficients, including Pearson, Spearman, and Kendall's Tau, to assess the relationships between thermal properties and compositional changes in the plasma-treated textile sludge. These statistical methods were employed to quantify the strength and nature of the associations between variables, such as temperature variations and weight loss during thermal analysis. Additionally, anomaly detection techniques, including the Isolation Forest algorithm, were utilized to identify outliers in the dataset, providing deeper insights into unusual material behaviors under specific treatment conditions. Future research could focus on optimizing plasma treatment parameters to maximize the degradation efficiency of hazardous compounds while minimizing energy consumption. Additionally, exploring the scalability of this method for industrial applications and investigating its applicability to other types of industrial waste could broaden the impact of this technology. Further studies could also examine the long-term environmental effects of plasma-treated sludge when used in applications such as soil amendment or construction materials, ensuring that the benefits extend beyond immediate waste reduction.

### Acknowledgements

The authors thank the management of Sri Sivasubramaniya Nadar College of Engineering, Kalavakkam for the infrastructural support rendered for the present study. The authors would also like to thank Sophisticated Test & Instrumentation Centre – STIC (Cochin) for the characterization facility rendered.

### References

- Wang M, Mao M, Zhang M, Wen G, Yang Q, Su B & Ren Q, Highly efficient treatment of textile dyeing sludge by CO<sub>2</sub> thermal plasma gasification, *Waste Manag*, 90 (2019) 29.
- Berkun M, Aras E & Nemlioglu S, Disposal of solid waste in Istanbul and along the Black Sea coast of Turkey, *Waste Manag*, 25 (2005) 847.
- He M, Hu Z, Xiao B, Li J, Guo X, Luo S, Yang F, Feng Y, Yang G & Liu S, Hydrogen-rich gas from catalytic steam gasification of municipal solid waste (MSW): Influence of catalyst and temperature on yield and product composition, *Int J Hydrog Energy*, 34 (2009) 195.
- Lemmens B, Elslander H, Vanderreydt I, Peys K, Diels L, Oosterlinck M & Joos M, Assessment of plasma gasification of high caloric waste streams, *Waste Manag*, 27 (2007) 1562.
- Gomez E, Rani D A, Cheeseman C R, Deegan D, Wise M & Boccaccini A R, Thermal plasma technology for the treatment of wastes: A critical review, *J Hazard Mater*, 161 (2009) 614.
- Laly L G & Ramachandran K, Modelling of transferred arc inside the crucible with gas injection through hollow cathode, *ACS Appl Mater Interf*, 10 (2018) 22408.
- Katou K, Asou T, Kurauchi Y & Sameshima R, Melting municipal solid waste incineration residue by plasma melting furnace with a graphite electrode, *Thin Solid Films*, 386 (2001) 183.
- Lapa N, Santos O J F, Camacho S L & Circeo L J, An ecotoxic risk assessment of residue materials produced by the plasma pyrolysis/vitrification (PP/V) process, *Waste Manag*, 22 (2002) 335.
- Jian-Jun H, Jia-Biao S, Rong-Qing L & Zheng-Zhi L, A new waste disposal technology-plasma arc pyrolysis system, *Plasma Sci Technol*, 5 (2003) 1743.
- Moustakas K, Fatta D, Malamis S, Haralambous K & Loizidou M, Demonstration plasma gasification/vitrification system for effective hazardous waste treatment, *J Hazard Mater*, 123 (2005) 120.
- Zhang Q, Wu Y, Dor L, Yang W & Wlodzimierz B, A thermodynamic analysis of solid waste gasification in the plasma gasification melting process, *Appl Energy*, 112 (2013) 405.
- Seok-Wan K, Hyun-Seo P & Hyung-Jin K, 100 kW steam plasma process for treatment of PCBs (Polychlorinated biphenyls) waste, *Vacuum*, 70 (2003) 59.
- Zhang Q, Dor L, Fenigshtein D, Yang W & Blasiak W, Gasification of municipal solid waste in the plasma gasification melting process, *Appl Energy*, 90 (2012) 106.
- Falcucci G, Jannelli E, Minutillo M, Ubertini S, Han J, Yoon S P & Nam S W, Integrated numerical and experimental study of a MCFC-plasma gasifier energy system, *Appl Energy*, 97 (2012) 734.
- Yang W, Ponzio A, Lucas C & Blasiak W, Performance analysis of a fixed-bed biomass gasifier using high-temperature air, *Fuel Process Technol*, 87 (2006) 235.
- Young L & Pian C C P, High-temperature, air-blown gasification of dairy-farm wastes for energy production, *Energy*, 28 (2003) 655.
- Veziroğlu T N & Şahin S, 21st century's energy: Hydrogen energy system, *Energy Convers Manag*, 49 (2008) 1820.
- Wang Q, Yan J H, Chi Y, Li X D & Lu S Y, Application of thermal plasma to vitrify fly ash from municipal solid waste incinerators, *Chemosphere*, 78 (2010) 626.
- Min T J, Yoshikawaand K & Murakami K, Distributed gasification and power generation from solid wastes, *Energy*, 30 (2005) 2219.
- Szargut J, Exergy in the thermal systems analysis In: Bejan A & Mamut E. (Eds) Thermodynamic optimization of complex energy systems, theory and practices for energy education, Training, Regulation and Standards, 69 (1999) 1.
- Hariri S, Kind M C & Brunner R J, Extended Isolation Forest, *IEEE Trans Knowl Data Eng*, 33 (2021) 1479.
- Karczmarek P, Kiersztyn A, Pedrycz W & Al E, K-means-based isolation forest, *Knowl Based Syst*, 195 (2020) 1.
- Li C, Guo L, Gao H & Li Y, Similarity-measured isolation forest: Anomaly detection method for machine monitoring data, *IEEE Trans Instrum Meas*, 70 (2021) 1.
- Xu D, Wang Y, Meng Y & Zhang Z, An improved data anomaly detection method based on isolation forest', Proceedings - 2017 10th International Symposium on Computational Intelligence and Design, ISCID 2017, 2 (2018) 287.
- Tokovarov M & Karczmarek Paweł, A probabilistic generalization of isolation forest, *Inf Sci*, 584 (2022) 433.